Collision-Energy-Resolved Penning Ionization Electron Spectroscopy of Thiazole and Benzothiazole: Study of Ionic States and Anisotropic Interactions between a Metastable He*(2^3S) Atom and Hetero Cyclic Compounds

Masakazu Yamazaki, Naoki Kishimoto, and Koichi Ohno*

Department of Chemistry, Graduate School of Science, Tohoku University, Aramaki, Aoba-ku, Sendai 980-8578, Japan

Received: March 14, 2006; In Final Form: April 7, 2006

Anisotropic interactions between a metastable He*(2^3S) atom and aromatic heterocyclic compounds (thiazole and benzothiazole) as well as their electronic structures were studied by means of collision-energy/electron-energy resolved two-dimensional Penning ionization electron spectroscopy combined with ab initio molecular orbital calculations. Different collision-energy dependence of partial ionization cross sections (CEDPICS) were clearly observed for different ionic states depending on anisotropic extents of molecular orbitals from which an electron is removed. It was found that thiazole and benzothiazole most strongly attract a He*(2^3S) atom around the region where the nitrogen lone pair orbital extends. For another heteroatom, sulfur, it is relatively weak, but a certain attractive interaction was found for the directions perpendicular to the molecular plane. Benzothiazole was shown to widely attract a He*(2^3S) atom in the out-of-plane directions, since the benzene moiety showed a deeper potential well than the five-membered ring. Assignments of the ionic states including shake-up states were also discussed from observed CEDPICS and ab initio molecular orbital calculations. In particular, for the satellite bands, a negative collision energy dependence of the band intensity was well supported by a configuration-interaction calculation that assigns the satellite bands to be the ionization from π orbitals accompanying $\pi-\pi^*$ or $n-\pi^*$ excitations.

I. Introduction

Heterocyclic compounds[1] play a major part in biological systems, and they can be found in such as DNA bases, amino acids, and vitamins, and so on. Thiazole and its benzene-condensed form, benzothiazole, are one of the simplest heterocycles which are often used as parent materials for a numerous of chemical compounds. To understand physical, chemical, and biological properties of heterocycles with a microscopic level, electronic structures and molecular orbital energies as well as how they interact with other species must be elucidated. Electronic structures of thiazole and benzothiazole were extensively studied by using ultraviolet photoelectron spectroscopy.[2−8] However, inconsistent assignments of ionic states were found partly because the assignments were made by the assumption based on the band shape or by the limited level of calculations in previous studies.[2−8]

Although localized interaction around a specific atom or functional group with other molecules plays an important role in connection with biological properties, anisotropic nature of intermolecular interactions is in general difficult to be investigated by experiments. In particular, in thiazole and benzothiazole, the directions of attractive sites on the N and S atoms are expected to be different from each other. Two-dimensional Penning ionization electron spectroscopy has been shown to be one of the most powerful methods to study anisotropic interactions between a metastable helium atom and a target molecule.[9−11] When a metastable helium atom, He*(2^3S), collides with a target molecule M, where He*(2^3S) has an excitation energy (E(He*(2^3S)) = 19.82 eV) larger than the lowest ionization potential (IP) of M, a chemiionization process known as Penning ionization[12] can occur:

$$\mathrm{He^*}(2^3\mathrm{S}) + \mathrm{M} \rightarrow \mathrm{He}(1^1\mathrm{S}) + \mathrm{M}_i^+ + e^- \qquad (1)$$

On the basis of the electron exchange model[13] proposed for the Penning ionization process, an electron in a molecular orbital (MO) of M is transferred to the inner-shell orbital of He* and the excited electron in He* is ejected, and thus the ionization into a final ionic state i takes place with a high probability when the 1s orbital of the He atom overlaps effectively with the target MO from which an electron is removed. Therefore, the reactivity of Penning ionization is directly related to the electron distribution of the ionized MO.[14]

When an electron spectroscopic technique is applied to Penning ionization, Penning ionization electron spectra (PIES),[15−18] which usually shows band intensities, widths, and positions different from those of ultraviolet photoelectron spectra (UPS), is obtained. Coupled experimental techniques including velocity (or collision energy) selection of He*(2^3S) atoms and electron kinetic energy analysis have been developed[9] to yield collision-energy/electron-energy resolved two-dimensional Penning ionization electron spectra (2D-PIES).[10] Collision energy dependence of partial ionization cross section (CEDPICS) obtained from 2D-PIES has been shown to reflect the interactions around the regions where the ionized MO mainly extends, because the most reactive geometries for Penning ionization are governed by the electron distributions of the target MOs.

It is known that a He*(2^3S) atom behaves similar to a Li(2^2S) atom in interactions with various kinds of atoms.[19−21] The

* To whom correspondence should be addressed. E-mail: ohnok@qpcrkk.chem.tohoku.ac.jp.

10.1021/jp061573m CCC: $33.50
Published on Web 05/09/2006

shape of the velocity dependence of the total scattering cross section of He*(2^3S) by He, Ar, and Kr is very similar to that of Li,[19] and the location of a interaction potential well and its depth are also very similar for He*(2^3S) and Li(2^2S) in interaction with various targets.[20,21] This well-known similarity of a Rg* atom to a respective alkali atom has therefore an advantage in calculating anisotropic model potentials, and this has been successfully utilized to interpret the results of 2D-PIES for many molecules. Classical trajectory calculations on potential energy surface for N_2 and CH_3CN interacting with a Li atom well explained the experimental features of CEDPICS for N_2 + He*-(2^3S)[22] and CH_3CN + He*(2^3S).[23] The Li model potentials can also be modified in order to give quantitative agreement between observed and calculated CEDPICS.[24]

In this study, He*(2^3S) 2D-PIESs were measured for aromatic compounds with two different heteroatoms, thiazole and benzothiazole. Although five-[25] and six-membered[26] heterocyclic compounds have been extensively studied by collision energy resolved measurements, the already investigated molecules contain just one kind of heteroatom. Nitrogen-containing molecules are well-known to strongly attract a He*(2^3S) atom at the directions where the lone pair electrons extend.[26−28] On the other hand, sulfur-containing molecules often show attractive interactions for perpendicular directions of molecular axis or plane.[25,29−32] However, it has not been investigated how anisotropic interactions change when a molecule contains a nitrogen and a sulfur atoms at the same time. Furthermore, some shake-up process of ionization is strongly expected for the present heterocyclic molecules, since the satellite bands in the valence ionic region have been already observed for thiophene, pyrrole,[25] and azines.[26] From these points of view, the anisotropic interactions between a metastable helium atom He*(2^3S) and thiazole and benzothiazole have been investigated by means of 2D-PIES combined with the Li model potential calculations in this study. The shake-up states of thiazole were discussed on the basis of the slope of CEDPICS and theoretical calculations including many-body effects.

II. Experimental Section

The experimental apparatus used in the present study has been reported in previous papers.[9,28] He I ultraviolet photoelectron spectra (He I UPS) were measured by using the He I resonance photons (584 Å, 21.22 eV) produced by a discharge in pure helium gas. A metastable beam of He was produced by a nozzle discharge source, and the He*(2^1S) component was quenched by a water-cooled helium discharge lamp. The kinetic energy of electrons ejected during the Penning ionization or photoionization was measured by a hemispherical electrostatic deflection type analyzer using an electron collection angle 90° to the incident He*(2^3S) or photon beam. The transmission efficiency curve of the electron energy analyzer was determined by comparing our He I UPS data with those of Gardner and Samson[33] and Kimura et al.[34] The energy resolution of the electron energy analyzer was 60 meV estimated from the full width at half-maximum (fwhm) of the $Ar^+(^2P_{3/2})$ peak in the He I UPS. The background pressure in the reaction chamber was on the order of 10^{-7} Torr, and the experiments were performed under a sample pressure of ca. 2×10^{-5} Torr.

In collision-energy-resolved measurements, the metastable He*(2^3S) beam was modulated by a pseudorandom chopper[28] and then introduced into a collision cell located 504 mm downstream from the chopper disk. The time-of-flight (TOF) of He* from the chopper to the collision cell can be obtained by the Hadamard transformation[28] of time-dependent electron signals emitted from a stainless steel plate inserted into the collision cell, since TOF of secondary electrons from the metal surface to the detector are negligibly short in comparison with that of the He* atoms. The time-dependent Penning ionization electron signals of sample molecules $I_e(E_e, t)$ as functions of electron kinetic energy E_e and time t were converted to $I_e(E_e, \tau_{TOF})$ as functions of E_e and TOF of the He* beam by the Hadamard transformation. The $I_e(E_e, \tau_{TOF})$ can be led to $I_e(E_e, v_{He^*})$ as functions of E_e and velocity of He* atoms v_{He^*}. From the following equations, the 2D Penning ionization cross section $\sigma(E_e, v_r)$ was obtained

$$\sigma(E_e, v_r) = c\frac{I_e(E_e, v_{He^*})}{I_{He^*}(v_{He^*})}\frac{v_{He^*}}{v_r} \tag{2}$$

$$v_r = \sqrt{{v_{He^*}}^2 + \frac{3k_BT}{m}} \tag{3}$$

where c is a constant, v_r is the relative velocity averaged over the velocity of the target molecule, k_B is the Boltzmann constant, and T and m are the gas temperature and the mass of the target molecule, respectively. The cross section in eq 2 is normalized by using the velocity distribution of He* beam $I_{He^*}(v_{He^*})$. Finally, $\sigma(E_e, v_r)$ is converted to $\sigma(E_e, E_c)$ by the relation

$$E_c = \frac{1}{2}\mu {v_r}^2 \tag{4}$$

where μ is the reduced mass of the colliding system. Collision energy dependence of partial ionization cross sections (CEDPICS) $\sigma(E_c)$ can be obtained by integrating 2D-PIES cross sections $\sigma(E_e,E_c)$ over the E_e range related to each ionic state.

III. Calculations

All ab initio quantum chemical calculations were performed on the GAUSSIAN program.[35] As for interactions between He*-(2^3S) and target molecules, a ground-state Li atom instead of a He*(2^3S) atom can be used to calculate the approximate potentials V_{Li} for V^* based on the similarity between He*(2^3S) and Li(2^2S).[19−21] Li(2^2S) has the same outer valence electronic configuration as He*(2^3S) with a 2s electron that mainly contributes to the interactions. For atomic targets (H, Li, Na, K, and Hg), quantitative estimation of the well depth of the Li model potential was recently summarized to be in good agreement with the ratio of 1.1 to 1.2 with respect to He*(2^3S).[21] Model interaction potential energy V_{Li} can be obtained by the following manner.

$$V_{Li} = E_{MLi} - (E_M + E_{Li}) \tag{5}$$

E_{MLi}, E_M, and E_{Li} are the total energy of the supermolecule (MLi), the isolated molecule (M), and the isolated Li atom, respectively. The Li model interaction potential calculations were performed by the second-order Møller−Plesset perturbation theory (MP2) with the 6-311++G** basis set. The full counterpoise method[36] was employed to correct the basis set superposition error (BSSE). The molecular structures were fixed at the experimental or optimized equilibrium geometry; the geometry of a thiazole molecule was selected from microwave spectroscopic measurements,[37] and that of benzothiazole was determined by the geometry optimizations at MP2 with the 6-311++G** basis set.

Vertical ionization potentials were calculated by using outer-valence Green's function (OVGF)[38] method with the 6-311++G** basis sets in order to assign the ionic states of

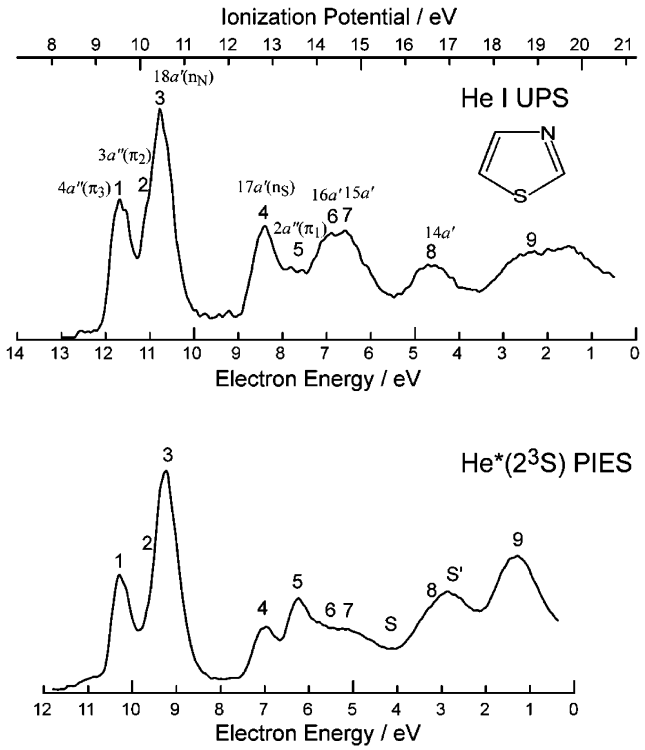

Figure 1. He I UPS and He* (2^3S) PIES of thiazole.

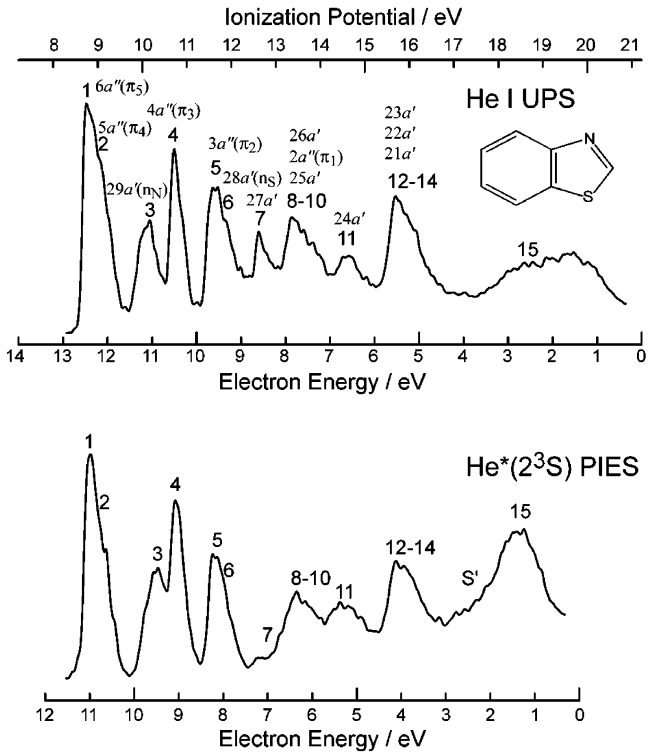

Figure 2. He I UPS and He* (2^3S) PIES of benzothiazole.

UPS and PIES. The symmetry-adapted-cluster (SAC)[39] symmetry-adapted-cluster configuration-interaction (SAC−CI)[40] calculations were also performed for the ionic states of thiazole by using the Ahlrichs VTZ basis[41] with d-type polarization functions of $\zeta_d = 0.75$, 0.80, 0.421 for C, N, and S atom, which were used in the SAC/SAC−CI study of five-membered heterocycles.[42] The general-*R* method was employed with the *R* operators up to triples. Electron distributions of molecular orbitals were also obtained by self-consistent field (SCF) calculations using the 6-311++G** basis sets.

IV. Results

Figures 1 and 2 show the He I UPS and the He*(2^3S) PIES of thiazole and benzothiazole, respectively. In UPS of thiazole, a very small signal probably originated from impurities was observed in both side of bands 1−3, but turned out to be much smaller in PIES. For comparison, the electron energy axes for PIES are shifted relative to those for UPS by the difference in excitation energies, 21.22−19.82 eV.

Figures 3 and 4 show collision-energy-resolved PIES of thiazole and benzothiazole, respectively. In each figure, the lower-collision-energy spectrum is shown by a broken line and the higher-collision-energy spectrum is shown by a solid line. Figures 5 and 6 show CEDPICS of thiazole and benzothiazole. The CEDPICS was obtained by integrating electron counts of the 2D-PIES over a proper E_e range of the ionic state and shown by log σ − log E_c plots in the E_c range of 90−300 meV for thiazole and of 90−280 meV for benzothiazole. Thin lines in the CEDPICS represent the least-squares-fitted lines. The calculated electron density maps for the respective MOs and simplified diagrams representing atomic orbital components of the MOs are also drawn in the figures. Thick solid line in the MO maps represents the molecular surface estimated from van der Waals radii of component atoms.

Tables 1 and 2 summarize the vertical IPs determined from He I UPS, the calculated IPs by the OVGF method, and the

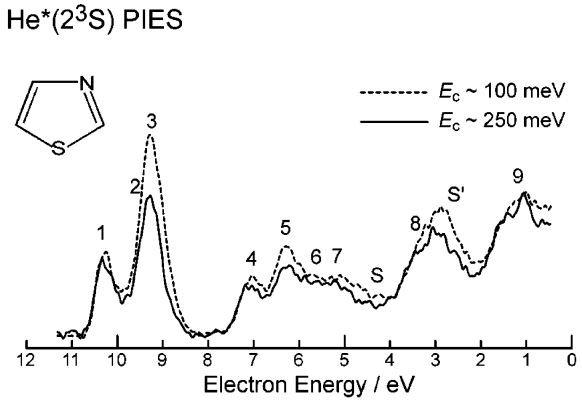

Figure 3. Collision-energy-resolved He*(2^3S) PIES of thiazole: broken curve, $E_c \sim 91-111$ meV (average 100 meV); solid curve, $E_c \sim 216-296$ meV (average 250 meV).

assignment of the observed bands. Some IP_{obsd}s were shown in parentheses, since their uncertainties are relatively large because of band overlapping and diffuseness. The peak energy shifts (ΔE) in PIES measured with respect to the "nominal" energy E_0 (E_0 = the difference between the metastable excitation energy and the target IP) are also shown in the tables. Values of the slope parameters *m* for the logσ−log E_c plots were estimated by a linear least-squares method. Because of band overlapping, some ΔE were not estimated and some *m* were listed in parentheses.

Figures 7 and 8 show interaction model potential energy curves between a Li atom and thiazole and benzothiazole, respectively. Potential energy curves are shown for (a) in-plane access of Li to the S, N, and H atoms and for (b) out-of-plane access to the S atom, the center of the five-menbered ring, or the benzene ring. For the in-plane access to the C−H bond, the direction was chosen as those where the highest σ_{CH} orbital (16a′ of thiazole and 27a′ of benzothiazole) mainly extends.

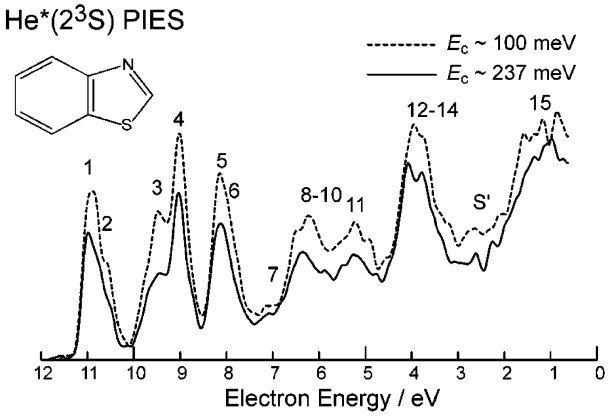

Figure 4. Collision-energy-resolved He*(2^3S) PIES of benzothiazole: broken curve, $E_c \sim 88-115$ meV (average 100 meV); solid curve, $E_c \sim 196-294$ meV (average 237 meV).

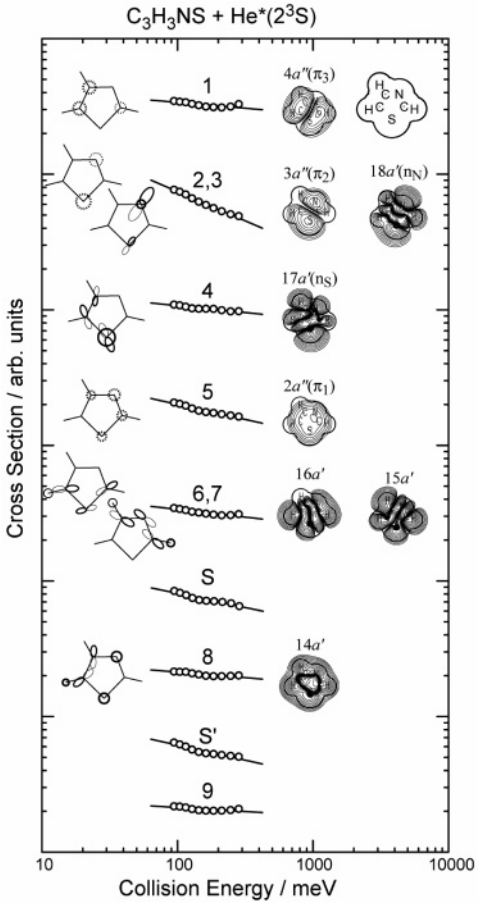

Figure 5. Collision energy dependence of partial ionization cross sections for thiazole by a collision with He*(2^3S). Electron density contour maps of a′ orbitals are plotted on the molecular plane; those of a″ orbitals are plotted on the plane above 1.7 Å from the molecular plane.

Table 3 lists the calculated ionization potentials and the corresponding electronic configurations obtained by the SAC/SAC−CI general-*R* method.

V. Discussion

A. Thiazole. Since the Penning ionization probability is mainly governed by the overlap between He 1s orbital and the MO from which an electron is removed, the ionization into the corresponding ionic state can effectively occur when a He* atom goes through the region where the MO has high electron density. As discussed in previous papers,[9,11,16] positive or negative slope of CEDPICS reflects the type and strength of interaction. In the case where the attractive interaction is dominant, slower He* atoms can approach the high electron density region more effectively through deflection of its trajectory. In this case, the collision with a large impact parameter dominantly contributes to the ionization cross section. When a He* atom has an enough speed to overcome the attractive force, a He* atom and a target molecule cannot be close to each other effectively. Niehaus[16]

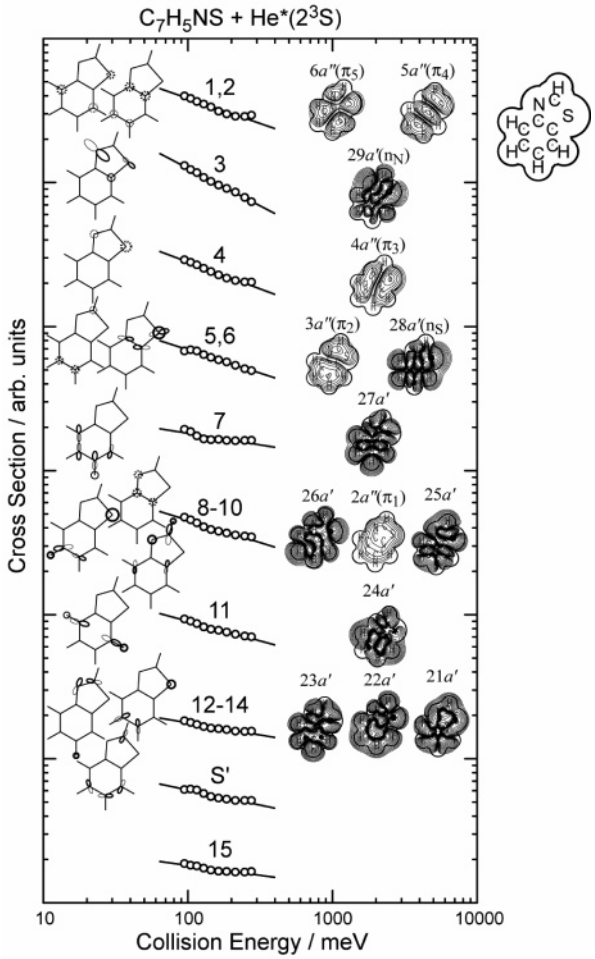

Figure 6. Collision energy dependence of partial ionization cross sections for benzothiazole by a collision with He*(2^3S). Electron density contour maps of a′ orbitals are plotted on the molecular plane; those of a″ orbitals are plotted on the plane above 1.7 Å from the molecular plane.

TABLE 1: Band Assignments, Observed Ionization Potential (IP_{obsd}), Calculated Ionization Potential (IP_{calcd}), Peak Energy Shift (ΔE), and Obtained Slope Parameter (m) of the logσ − log E_c Plots in CEDPICS for Thiazole (See Text)

band	orbital character	IP_{obsd}/eV	IP_{calcd} [a]/eV	ΔE/meV	m
1	4a″ (π_3)	9.54	9.534 (0.90)		−0.09
2	3a″ (π_2)	(10.2)	10.367 (0.89)		(−0.43)
3	18a′ (n_N)	10.46	10.504 (0.89)	−120	(−0.43)
4	17a′ (n_S)	12.82	12.883 (0.89)		−0.10
5	2a″ (π_1)	(13.5)	13.902 (0.82)		−0.22
6	16a′ (σ)	14.34	14.378 (0.89)		(−0.11)
7	15a′ (σ)	14.64	14.951 (0.89)		(−0.11)
S		(~15.6)			−0.21
8	14a′ (σ)	(16.6)	17.024 (0.85)		−0.08
S′		(~17.1)			−0.22
9		(18.9)			−0.06

[a] The pole strength in parentheses.

TABLE 2: Band Assignments, Observed Ionization Potential (IP_{obsd}), Calculated Ionization Potential (IP_{calcd}), Peak Energy Shift (ΔE), and Obtained Slope Parameter (m) of the logσ − log E_c Plots in CEDPICS for Benzothiazole (See Text)

band	orbital character	IP_{obsd}/eV	IP_{calcd}[a]/eV	ΔE/meV	m
1	6a″ (π_5)	8.74	8.857 (0.88)	−90	(−0.35)
2	5a″ (π_4)	(9.0)	8.891 (0.88)		(−0.35)
3	29a′ (n_N)	10.18	10.437 (0.88)	−190	−0.52
4	4a″ (π_3)	10.72	10.726 (0.87)		−0.37
5	3a″ (π_2)	(11.7)	11.807 (0.82)		(−0.33)
6	28a′ (n_S)	(11.9)	12.069 (0.89)		(−0.33)
7	27a′ (σ)	12.62	12.961 (0.88)		−0.16
8	26a′ (σ)	13.36	13.630 (0.87)		(−0.31)
9	2a″ (π_1)		13.992 (0.80)		(−0.31)
10	25a′ (σ)		14.105 (0.87)		(−0.31)
11	24a′ (σ)	(14.7)	14.985 (0.87)		−0.27
12	23a′ (σ)	15.69	16.146 (0.85)		(−0.17)
13	22a′ (σ)		16.345 (0.84)		(−0.17)
14	21a′ (σ)		16.392 (0.84)		(−0.17)
S′		(∼17.3)			−0.21
15		(18.7)			−0.14

[a] The pole strength in parentheses.

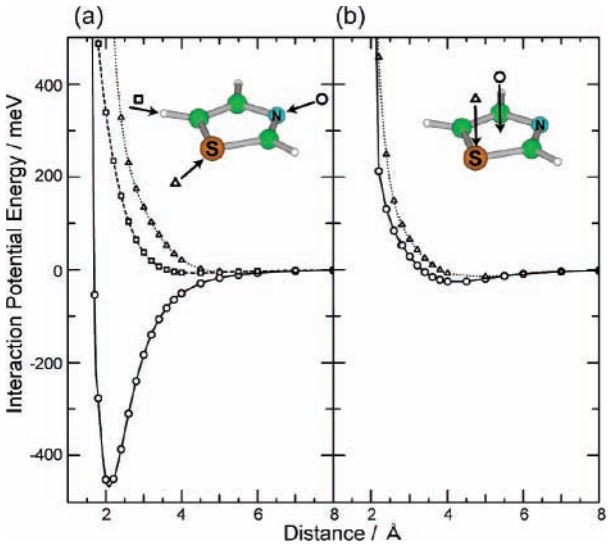

Figure 7. Interaction model potential curves between a Li atom and a thiazole molecule for (a) the in-plane and (b) the out-of-plane accesses of a Li atom.

showed collision energy dependence of ionization cross section for atomic targets by using classical relations. If the long-range attractive part of the interaction potential $V^*(R)$ plays a dominant role for collision dynamics, and its functional form is of the type

$$V^*(R) \propto R^{-s}, \tag{6}$$

collision energy dependence of the cross section $\sigma(E_c)$ can be represented by

$$\sigma(E_c) \propto E_c^{-2/s} \tag{7}$$

Therefore, the slope m of the log σ − log E_c plots can be related to the steepness of the attractive part of the interaction potential ($m = -2/s$).

For thiazole and benzothiazole, various m values were observed according to the direction where the ionized MO is mainly extending. The a″ (π-type) orbitals extend perpendicular directions to the molecular plane, whereas the a′ (σ-type) orbitals extend on the molecular plane. There are also lone-pair type

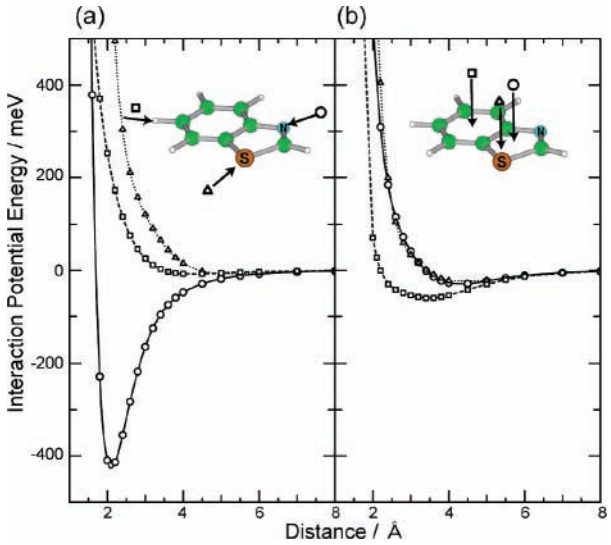

Figure 8. Interaction model potential curves between a Li atom and a benzothiazole molecule for (a) the in-plane and (b) the out-of-plane accesses of a Li atom.

orbitals with the a′ symmetry in which the electrons are localized around the nitrogen (n_N) or sulfur (n_S) atom.

For thiazole, the largest negative slope of CEDPICS ($m = -0.43$) was observed for the second and the third ionic states which correspond to the ionization of 3a″ (π_2) and 18a′ (nitrogen lone pair; n_N) orbitals, respectively. Although the bands 2 and 3 are strongly overlapping as shown in Figure 1, the ordering in IPs for the bands 2 and 3 of UPS was determined as 3a″ (π_2) < 18a′(n_N) based on the vibrational fine structures in UPS,[8] and the present OVGF calculations resulted in a consistent assignment with previous studies.[4,8] As shown in Figure 5, the 3a″ (π_2) orbital mainly consists of the sulfur 3p orbital (S_{3p}) whose lobe is extending to the perpendicular direction to the molecular plane. Therefore, the slope value of $m = -0.43$ for the second and third ionic states can indicate the averaged attractive force around the different two regions; in-plane directions where the n_N orbital distributes and out-of-plane directions where the sulfur 3p orbital is extending. The Li model interaction potentials (Figure 7a) indicate that the strong attractive interactions with the well depth of ca. 450 meV occur when a He* atom approaches the region where the n_N orbital is extending. Therefore, the largest negative slope of CEDPICS for the bans 2 and 3 ($m = -0.43$) is attributed to ionization from the n_N orbital.

From Figure 5 and Table 1, the difference in slope values among π bands can be noticed. The order of the slope values of CEDPICS for three π bands is π_2 ($m = -0.43$) > π_1 ($m = -0.22$) > π_3 ($m = -0.09$), although the slope value for the π_2 band must be strongly affected by that for the n_N band. The strength of attractive interactions around π orbitals may be interpreted by the contribution of the sulfur 3p (S_{3p}) atomic orbital component to π orbitals. As can be seen in the diagram inserted in Figure 5, the π_1 orbital contains the S_{3p} component to a certain extent, whereas the π_3 orbital almost consists of carbon 2p orbitals. From the model interaction potentials in Figure 7b, attractive interaction with a well depth of ca. 15 meV can be found for the out-of-plane access of a Li atom to the sulfur atom. Therefore, the weak attractive interaction region above the five-membered ring extends to the sulfur atom. This relation between the negative slope values and the S_{3p} components was also observed in the 2D-PIES study of thiophene.[25] In the case of thiophene, the slope values of CEDPICS for the

TABLE 3: Observed Ionization Potential (IP_{obsd}), Calculated Ionization Potential (IP_{calcd}), and Main Configuration for the Ionized States of Thiazole (See Text)

band	orbital character[a]	IP_{obsd}/eV	IP_{calcd} [b]/eV	main configuration
1	$4a''(\pi_3)$	9.54	9.17	$0.96(4a''^{-1})$
2	$3a''(\pi_2)$	(10.2)	10.12	$0.95(3a''^{-1})$
3	$18a'(n_N)$	10.46	10.10	$0.93(18a'^{-1})$
4	$17a'(n_S)$	12.82	12.88	$0.94(17a'^{-1})$
5	$2a''(\pi_1)$	(13.5)	13.63	$0.89(2a''^{-1})$
6	$16a'(\sigma)$	14.34	14.28	$0.93(16a'^{-1})$
7	$15a'(\sigma)$	14.64	14.76	$0.94(15a'^{-1})$
S	−	(∼15.6)	16.75	$0.85(4a''^{-2}5a''^{1})$
			16.92	$0.91(18a'^{-1}5a''^{1}4a''^{-1}) + 0.59(4a''^{-1}5a''^{1}18a'^{-1}) - 0.45(14a'^{-1})$
8	$14a'(\sigma)$	(16.6)	17.01	$0.78(14a'^{-1}) + 0.55(18a'^{-1}5a''^{1}4a''^{-1})$
S′	−	(∼17.1)	17.93	$0.91(3a''^{-1}5a''^{1}4a''^{-1}) + 0.62(4a''^{-1}5a''^{1}3a''^{-1})$
			18.19	$0.80(18a'^{-1}6a''^{1}4a''^{-1}) + 0.67(4a''^{-1}6a''^{1}18a'^{-1})$
			18.70	$0.63(4a''^{-1}5a''^{1}3a''^{-1}) - 0.56(4a''^{-2}6a''^{1})$
9	−	(18.9)	18.85	$0.78(13a'^{-1})$

[a] Orbital character is taken from Table 1. [b] Calculated by SAC/SAC−CI general-*R* method.

observed three π bands were $m(\pi_2) = -0.40 < m(\pi_1) = -0.33 < m(\pi_3) = -0.26$, which was the same order as the magnitude of the S_{3p} atomic orbital component.

The ionization cross sections for σ bands showed relatively small negative dependence on collision energy. As discussed in the literature,[16] if the repulsive part of the interaction potential becomes dominant for the energy dependence, the slope value of $\log \sigma - \log E_c$ for an atomic target can be expressed as

$$m \approx \frac{B}{D} - \frac{1}{2} \tag{8}$$

where D and B are the decay parameters of the repulsive potential ($V^*(R) \propto \exp(-DR)$) and of the transition probability ($W(R) \propto \exp(-BR)$), respectively. A soft repulsive wall generally gives an increase in the ionization cross section with collision energy. However, a steep repulsive wall (large D) compared to the steepness of the transition probability can lead a smaller (B/D) value than $^1/_2$ and a weak negative dependence. For thiazole, a small negative dependence for bands 6 and 7 ($m = -0.11$) and band 8 ($m = -0.08$), which are related to the ionization from the σ_{CH} orbitals, can be ascribed to the influence of both the repulsive potential around the σ_{CH} orbital region and the attractive potential around the nitrogen or the perpendicular directions to the ring on average. The interaction potential of in-plane directions around the sulfur atom may also be repulsive, which is indicated by the model potential calculations in Figure 7a. The band 4 of thiazole, which corresponds to the ionization from $17a'$ (n_S) orbital, showed a weak negative collision energy dependence, and the slope value ($m = -0.10$) is comparable to those of the σ_{CH} bands. Therefore, strongly attractive interaction region for the in-plane direction must be almost localized around the N atom.

Anisotropic characteristics of the interaction potential investigated in the present study are consistent with the previous studies on nitrogen- or sulfur-containing compounds. Interactions around the area where a nitrogen lone-pair orbital is extending are known to be strongly attractive.[26−28] For nitriles (propionitrile, acrylonitrile, and 3-butenenitrile), the CEDPICS for the ionization from the nitrogen lone-pair orbital gave the slope values from −0.48 to −0.60.[28] The slope value of −0.54 was obtained for the CEDPICS of the ionization from the n_N orbital of pyridine,[26] which is comparable to the result in this study; $m = -0.43$ for the bands 2 and 3 of thiazole, and $m = -0.52$ for the band 3 of benzothiazole, which will be discussed in section V−B. For sulfur-containing compounds,[29−32] attractive interaction was also found for the vertical direction to the C−S or the C═S bond similarly to the present case. However, in thiophene, the slope values of CEDPICS for the π band ranged from −0.26 to −0.40, while much smaller values were obtained for thiazole ($m = -0.09$ and −0.22 for the π_3 and π_1 bands, respectively). This fact is consistent with the attractive well depth by Li model potentials, since the well depth (25 meV) for the perpendicular direction to the molecular plane of thiazole (marked with circle in Figure 7b) is shallower than that of thiophene (> 100 meV).

B. Benzothiazole. In the case of benzothiazole, the ionizations from $29a'$ (n_N, band 3) and $4a''$ (π_3, band 4) orbitals were observed as well separate bands to each other. Although the Koopmans' theorem gives inversed IP order for the $29a'$ (n_N) (12.003 eV) and the $4a''$ (π_3) (11.476 eV) orbitals, the present OVGF calculations resulted in consistent assignments with previous studies[5,7,8] and with the results of CEDPICS in this study. The CEDPICS for the ionization from the n_N orbital showed much larger negative slope ($m = -0.52$) than that for the ionization from the π_3 orbital ($m = -0.37$). As with the case of thiazole, the deepest point (ca. 420 meV) of the attractive well is found for the in-plane access of Li atom to the N atom. Therefore, the slope value of the CEDPICS for the overlapping bands 2 and 3 of thiazole ($m = -0.43$) can be recognized as nearly the average value of $m = -0.52$ (n_N) and −0.37 (π_3), which were observed for the ionizations from the n_N orbital and the S_{3p} orbital in benzothiazole, respectively.

The bands 1, 2, and 4 contain the ionizations only from the π orbitals. In the case of benzothiazole, the same trend as in the case of thiazole may be noticed for the different slope values of CEDPICS for π bands. The CEDPICS for the ionization from the $4a''$ (π_3;S_{3p}) orbital (band 4) shows the largest negative slope value ($m = -0.37$) among five π bands. The $6a''$ (π_5) orbital has also the sulfur 3p component and thus the CEDPICS for bands 1 and 2 gives the next largest negative slope ($m = -0.35$). Although slope values for other π bands could not be obtained separately, the π-ionization dynamics is mostly governed by the attractive interactions along the perpendicular directions to the molecular plane around the sulfur atom. However, the effect of the benzene ring can be noticed if the absolute slope values for π bands are compared between thiazole and benzothiazole. Benzene is known to attract a He* atom around the region where π electrons distribute.[43] The Li model potential calculations for benzothiazole also resulted in a certain attractive well (ca. 60 meV) for out-of-plane access of a Li atom to the benzene ring. Since the well depth (ca. 30 meV) for the access to the five-membered ring of benzothiazole is comparable to that of thiazole (ca. 25 meV), the larger negative CEDPICS for π bands of

benzothiazole than those for thiazole can be interpreted as the effect of attractive interactions around the benzene moiety.

Although the slope values of CEDPICS well provide us with information on anisotropic interactions between He*(2^3S) and target molecules, peak energy shifts in PIES should be discussed here. The largest negative shift in peak position was clearly observed for ionization from the n_N band (band 3 of thiazole and benzothiazole), which is consistent with the preceding discussion. Although peak energy shifts with absolute values smaller than 50 meV were not shown in Tables 1 and 2, next largest negative shift was found for π bands ($\Delta E(\pi_5) = -90$ meV for benzothiazole, and $\Delta E(\pi_1) = -80$ meV for thiazole which is not shown in Table 1 because of uncertainty in estimating the peak position in UPS.). For weakly attractive interactions, anisotropic characteristics can be well studied by different behavior of CEDPICS, however, the absolute value of interaction energy is difficult to be estimated from peak energy shift, which was the case with benzene where $\pi_3 \sim \pi_1$ bands showed small negative shift with a large uncertainty ($\Delta E(\pi_3,\pi_2) = -80 \pm 70$ meV and $\Delta E(\pi_1) = -70 \pm 70$ meV).[44]

For in-plane directions where σ_{CH} orbitals extend, relatively smaller slope values of CEDPICS than those for π bands were observed, which is again due to repulsive interaction for the directions. As can be seen in Figure 8a, the Li model potentials well support the experimental results. Although the n_S band of benzothiazole could not be separated from π_2 band, repulsive interactions for in-plane access of He* to the S atom is also expected by both of the result of CEDPICS and the model potentials.

C. Electronic Structure and Satellite Bands Observed in PIES. It is generally difficult to assign the ionization from π orbitals in the binding energy region of 11−15 eV, because σ bands are observed to be considerably overlapping with π bands in that region. However, PIES band intensity and its collision energy dependence were shown to be useful to make assignment. It is well-known that the π bands are strongly enhanced in PIES because of large extending π orbitals, which enables us to know about interactions around the region where π electrons are distributed. In the previous UPS studies for thiazole,[8] band 5 was assumed to be the ionization from a σ orbital because of the band broadness and the unreliability of semiempirical calculations. However, band 5 in PIES of thiazole shows stronger intensity than the band 4 and the bands 6 and 7, and the present OVGF calculation showed that the fifth ionic state corresponds to the ionization from the π_1 orbital. Negative collision-energy dependence of the band 5 ($m = -0.22$) is also consistent with ionization from π_1 orbital. For benzothiazole, it is difficult to make a detail assignment for the ionization from the 2a″ (π_1) orbital, because the OVGF method gave nearly the same IP values for the 2a″ (π_1) and 25a′ (σ) orbitals. The slope value ($m = -0.31$) of the CEDPICS for bands 8−10, however, suggests that the ionic state for ionization from the π_1 orbital should be appeared within the bands. For benzothiazole, it is also notable that the band 7 has a weak intensity in PIES, since the corresponding 27a′ (σ) orbital localizes around the σ_{CH} bonds of the six-membered ring.

In CERPIES of thiazole and benzothiazole (Figures 3 and 4), a certain negative collision-energy dependence can be noticed in the electron energy regions around ∼4.25 eV (IP ∼ 15.6 eV) and around ∼3−2 eV (IP ∼ 17.3 eV) which are denoted as S and S′, respectively. The slope values of the CEDPICS for the S band ($m = -0.21$) and the S′ band ($m = -0.22$ for thiazole and $m = -0.21$ for benzothiazole) may enable us to relate them to the slope for π bands, since the slopes can be distinguished from those for the neighboring σ bands. The SAC/SAC−CI general-*R* calculation was performed for the ionic states of thiazole, and the results are listed in Table 3. Some satellite shake-up states are found in the IP region larger than 16 eV. Two shake-up states were calculated around the S band, and they mainly correspond to the ionization from 4a″ (π_3) orbitals accompanying the HOMO (4a″,π_3) − LUMO (5a″,π_4) or the 18a′(n_N) − LUMO (π_4) excitations. Three shake-up states were also found between band 8 and 9, which corresponds to the S′ band. S′ is found to be consist of the ionization from the π_3, π_2, or n_N orbitals leading to the $\pi-\pi^*$ or $n-\pi^*$ excitations. Therefore, the relatively larger negative slope value for S and S′ bands than those for σ_{CH} bands was mainly due to the ionization from π orbitals (HOMO or next-HOMO) accompanying the $\pi-\pi^*$ or $n-\pi^*$ excitations.

VI. Conclusion

Anisotropic interactions of thiazole and benzothiazole with a metastable He*(2^3S) atom were investigated by collision-energy/electron-energy-resolved two-dimensional Penning ionization electron spectroscopy combined with ab initio model interaction potential calculations. Observed partial ionization cross sections showed different collision energy dependence depending on the spatial region where the ionized molecular orbital extends. The following remarks can be made from observation of the slopes in the log−log plot of collision energy dependence of partial ionization cross sections (CEDPICS).

(1) Thiazole and benzothiazole strongly attract a He*(2^3S) atom approaching the region where the nitrogen lone-pair orbital extends.

(2) Interactions for perpendicular directions to the molecular plane are also weakly attractive. The attractive interactions for the out-of-plane access of He*(2^3S) to the sulfur atom play an important role determining the slope of CEDPICS for π bands, since the magnitude of the sulfur atomic orbital component could account for the difference of the slope values among π bands.

(3) For benzothiazole, the benzene moiety more strongly attract a He*(2^3S) atom than the five-membered ring, which resulted in larger negative slope values of CEDPICS for π bands than those of thiazole.

(4) For in-plane access of He*(2^3S) to the investigated molecules, the interaction becomes repulsive type, except for the region where the nitrogen lone-pair orbital extends.

These experimental findings were well supported with ab initio model interaction potential calculations where a Li(2^2S) atom was used instead of a He*(2^3S) atom.

In concerning with electronic structures, the band intensities and the slope values of CEDPICS were shown to be useful to make assignment of ionic states. It was found in PIES that relatively larger negative collision energy dependence was embedded in the electron energy region below 5 eV. The slope values of CEDPICS for the satellite bands were related to the ionization from π orbitals. From the SAC/SAC−CI general-*R* method, the satellite bands were well assigned as the shake-up states in which the highest- or next-highest π orbitals are ionized accompanying the $\pi-\pi^*$ or $n-\pi^*$ excitations.

Acknowledgment. The present work was supported by a Grant-in-Aid for Scientific Research from the Japanese Ministry of Education, Culture, Sports, Science and Technology. M.Y. is supported by the Research Fellowships of the Japan Society for the Promotion of Science for Young Scientists.

References and Notes

(1) Balaban, A. T.; Oniciu, D. C.; Katritzky, A. R. *Chem. Rev.* **2004**, *104*, 2777.

(2) Eland, J. H. D. *Int. J. Mass Spectrom. Ion Phys.* **1969**, *2*, 471.
(3) Bernardi, F.; Forlani, L.; Todesco, P. E.; Colonna, F. P.; Distefano, G. *J. Electron Spectrosc. Relat. Phenom.* **1976**, *9*, 217.
(4) Palmer, M. H.; Findlay, R. H.; Ridyard, J. N. A.; Barrie, A.; Swift, P. *J. Mol. Struct.* **1977**, *39*, 189.
(5) Palmer, M. H.; Kennedy, S. M. F. *J. Mol. Struct.* **1978**, *43*, 203.
(6) Salmona, G.; Faure, R.; Vincent, E. J.; Guimon, C.; Pfister-Guillouzo, G. *J. Mol. Struct.* **1978**, *48*, 205.
(7) Guimon, C.; Pfister-Guillouzo, G.; Salmona, G.; Vincent, E. J. *J. Chim. Phys.* **1978**, *75*, 859.
(8) Rademacher, P.; Kowski, K.; Müller, A.; Bohlmann, G. *J. Mol. Struct.* **1993**, *296*, 115.
(9) Ohno, K.; Takami, T.; Mitsuke, K.; Ishida, T. *J. Chem. Phys.* **1991**, *94*, 2675.
(10) Ohno, K.; Yamakado, H.; Ogawa, T.; Yamata, T. *J. Chem. Phys.* **1996**, *105*, 7536.
(11) Ohno, K. *Bull. Chem. Soc. Jpn.* **2004**, *77*, 887.
(12) Penning, F. M. *Naturwissenschaften* **1927**, *15*, 818.
(13) Hotop, H.; Niehaus, A. *Z. Phys.* **1969**, *228*, 68.
(14) Ohno, K.; Mutoh, H.; Harada, Y. *J. Am. Chem. Soc.* **1983**, *105*, 4555.
(15) Čermák, V. *J. Chem. Phys.* **1966**, *44*, 3781.
(16) Niehaus, A. *Adv. Chem. Phys.* **1981**, *45*, 399.
(17) Yencha, A. J. *Electron Spectroscopy: Theory, Techniques, and Applications*; Brundle,C. R., Baker, A. D., Eds.; Academic: New York, 1984; Vol. 5.
(18) Siska, P. E. *Rev. Mod. Phys.* **1993**, *65*, 337.
(19) Rothe, E. W.; Neynaber, R. H.; Trujillo, S. *J. Chem. Phys.* **1965**, *42*, 3310.
(20) Haberland, H.; Lee, Y. T.; Siska, P. E. *Adv. Chem. Phys.* **1981**, *45*, 487.
(21) Hotop, H.; Roth, T. E.; Ruf, M.-W.; Yencha, A. J. *Theor. Chem. Acc.* **1998**, *100*, 36.
(22) Ogawa, T.; Ohno, K. *J. Chem. Phys.* **1999**, *110*, 3773.
(23) Ogawa, T.; Ohno, K. *J. Phys. Chem. A* **1999**, *103*, 9925.
(24) Maeda, S.; Yamazaki, M.; Kishimoto, N.; Ohno, K. *J. Chem. Phys.* **2004**, *120*, 781.
(25) Kishimoto, N.; Yamakado, H.; Ohno, K. *J. Phys. Chem.* **1996**, *100*, 8204.
(26) Kishimoto, N.; Ohno, K. *J. Phys. Chem. A* **2000**, *104*, 6940.
(27) Pasinszki, T.; Yamakado, H.; Ohno, K. *J. Phys. Chem.* **1995**, *99*, 14678.
(28) Kishimoto, N.; Aizawa, J.; Yamakado, H.; Ohno, K. *J. Phys. Chem. A* **1997**, *101*, 5038.
(29) Kishimoto, N.; Yokoi, R.; Yamakado, H.; Ohno, K. *J. Phys. Chem. A* **1997**, *101*, 3284.
(30) Kishimoto, N.; Furuhashi, M.; Ohno, K. *J. Electron Spectrosc. Relat. Phenom.* **2000**, *113*, 35.
(31) Kishimoto, N.; Osada, Y.; Ohno, K. *J. Phys. Chem. A* **2000**, *104*, 1393.
(32) Kishimoto, N.; Horio, T.; Maeda, S.; Ohno, K. *Chem. Phys. Lett.* **2003**, *379*, 332.
(33) Gardner, J. L.; Samson, J. A. R. *J. Electron Spectrosc. Relat. Phenom.* **1976**, *8*, 469.
(34) Kimura, K.; Katsumata, S.; Achiba, Y.; Yamazaki, T.; Iwata, S. *Handbook of He I Photoelectron Spectra of Fundamental Organic Molecules*; Japan Scientific: Tokyo, 1981.
(35) Frisch, M. J.; Trucks, G. W.; Schlegel, H. B.; Scuseria, G. E.; Robb, M. A.; Cheeseman, J. R.; Montgomery, J. A., Jr.; Vreven, T.; Kudin, K. N.; Burant, J. C.; Millam, J. M.; Iyengar, S. S.; Tomasi, J.; Barone, V.; Mennucci, B.; Cossi, M.; Scalmani, G.; Rega, N.; Petersson, G. A.; Nakatsuji, H.; Hada, M.; Ehara, M.; Toyota, K.; Fukuda, R.; Hasegawa, J.; Ishida, M.; Nakajima, T.; Honda, Y.; Kitao, O.; Nakai, H.; Klene, M.; Li, X.; Knox, J. E.; Hratchian, H. P.; Cross, J. B.; Adamo, C.; Jaramillo, J.; Gomperts, R.; Stratmann, R. E.; Yazyev, O.; Austin, A. J.; Cammi, R.; Pomelli, C.; Ochterski, J. W.; Ayala, P. Y.; Morokuma, K.; Voth, G. A.; Salvador, P.; Dannenberg, J. J.; Zakrzewski, V. G.; Dapprich, S.; Daniels, A. D.; Strain, M. C.; Farkas, O.; Malick, D. K.; Rabuck, A. D.; Raghavachari, K.; Foresman, J. B.; Ortiz, J. V.; Cui, Q.; Baboul, A. G.; Clifford, S.; Cioslowski, J.; Stefanov, B. B.; Liu, G.; Liashenko, A.; Piskorz, P.; Komaromi, I.; Martin, R. L.; Fox, D. J.; Keith, T.; Al-Laham, M. A.; Peng, C. Y.; Nanayakkara, A.; Challacombe, M.; Gill, P. M. W.; Johnson, B.; Chen, W.; Wong, M. W.; Gonzalez, C.; Pople, J. A. Gaussian 03, Revision C.02, Gaussian, Inc.: Wallingford CT, 2004.
(36) Boys, S. F.; Bernardi, F. *Mol. Phys.* **1970**, *19*, 553.
(37) Nygaard, L.; Asmussen, E.; Høg, J. H.; Maheshwari, R. C.; Nielsen, C. H.; Petersen, I. B.; Rastrup-Andersen, J.; Sørensen, G. O. *J. Mol. Struct.* **1971**, *8*, 225.
(38) (a) Ortiz, J. V. *J. Chem. Phys.* **1996**, *104*, 7599. (b) Ferreira, A. M.; Seabra, G.; Dolgounitcheva, O.; Zakrzewski, V. G.; Ortiz, J. V. *Understanding Chemical Reactivity, Vol. 22, Quantum-Mechanical Prediction of Thermochemical Data*; Cioslowski, J., Ed.; Kluwer: Dordrecht, The Netherlands, 2001; pp 131−160. (c) Ortiz, J. V. *Computational Chemistry: Reviews of Current Trends*; Leszczynski, J., Ed.; World Scientific: Singapore, 1997; Vol. 2, pp 1−61.
(39) Nakatsuji, H.; Hirao, K. *J. Chem. Phys.* **1978**, *68*, 2053.
(40) Nakatsuji, H. *Chem. Phys. Lett.* **1978**, *59*, 362.
(41) Schafer, A.; Horn, H.; Ahlrichs, R. *J. Chem. Phys.* **1992**, *97*, 2571.
(42) Ehara, M.; Ohtsuka, Y.; Nakatsuji, H.; Takahashi, M.; Udagawa, Y. *J. Chem. Phys.* **2005**, *122*, 234319.
(43) Yamazaki, M.; Maeda, S.; Kishimoto, N.; Ohno, K. *J. Chem. Phys.* **2005**, *122*, 044303.
(44) Yamakita, Y.; Yamauchi, M.; Ohno, K. *Chem. Phys. Lett.* **2000**, *322*, 189.